

# A Deep Learning Pipeline Using Synthetic Data to Improve Interpretation of Paper ECG Images

Xiaoyu Wang<sup>1</sup>, Ramesh Nadarajah<sup>2</sup>, Zhiqiang Zhang<sup>3</sup> David Wong<sup>1</sup>

<sup>1</sup>Leeds Institute of Health Sciences, University of Leeds, Leeds, UK, <sup>2</sup>Leeds Institute of Cardiovascular and Metabolic Medicine, University of Leeds, Leeds, UK, <sup>3</sup>School of Electronic and Electrical Engineering, University of Leeds, Leeds, UK

## Abstract

*Cardiovascular diseases (CVDs) are the leading global cause of death, and early detection is essential to improve patient outcomes. Electrocardiograms (ECGs), especially 12-lead ECGs, play a key role in the identification of CVDs. These are routinely interpreted by human experts, a process that is time-consuming and requires expert knowledge. Historical research in this area has focused on automatic ECG interpretation from digital signals, with recent deep learning approaches achieving strong results. In practice, however, most ECG data in clinical practice are stored or shared in image form. To bridge this gap, we propose a deep learning framework designed specifically to classify paper-like ECG images into five main diagnostic categories. Our method was the winning entry to the 2024 British Heart Foundation Open Data Science Challenge. It addresses two main challenges of paper ECG classification: visual noise (e.g., shadows or creases) and the need to detect fine-detailed waveform patterns. We propose a pre-processing pipeline that reduces visual noise and a two-stage fine-tuning strategy: the model is first fine-tuned on synthetic and external ECG image datasets to learn domain-specific features, and then further fine-tuned on the target dataset to enhance disease-specific recognition. We adopt the ConvNeXt architecture as the backbone of our model. Our method achieved AUROC scores of 0.9688 on the public validation set and 0.9677 on the private test set of the British Heart Foundation Open Data Science Challenge, highlighting its potential as a practical tool for automated ECG interpretation in clinical workflows.*

## 1. Introduction

The American Heart Association (AHA) estimates that, in 2024, 19.9 million people died from cardiovascular diseases (CVDs) [1]. CVDs are the leading cause of death, globally, and its prevalence is increasing [2].

Electrocardiograms (ECG), especially 12-lead ECG, have long been considered the gold standard for cardiac diagnostics, providing crucial information on cardiovascular conditions [3]. ECGs are usually interpreted by human clinical experts. However, manual analysis of ECGs can be time-consuming for clinicians [4]. Fast and accurate interpretation of ECGs to assist in diagnosis of CVDs improve patient outcomes and reduce health care costs by allowing earlier intervention.

Various machine learning and deep learning architectures, such as Deep Neural Network (DNN), Convolutional Neural Network (CNN), and Recurrent Neural Networks (RNN), have been applied to automatically interpret the ECGs [3, 5]. They have been used to detect atrial fibrillation [6–8], myocardial infarction [9, 10], and other abnormalities [11]. However, a major limitation is that they predominantly rely on digital ECG waveforms as input. In real-world clinical settings, especially in many hospitals and primary care facilities, most ECG data is still archived and shared on printed or scanned paper, rather than as raw digital signals [12].

To bridge this gap, we propose an artificial intelligence based method that aims to interpret paper ECGs and to make 5 types of important cardiovascular disease, including myocardial infarction, atrial fibrillation, hypertrophy, conduction disturbance, and ST/T change.

This task presents several challenges. First, paper ECG images often contain various types of noise and artefacts that are not present in clean digital waveforms. These include handwritten text, wrinkles, creases, and perspective transforms introduced during printing, scanning, or photographing. Such artefacts can obscure critical details and degrade the performance of traditional image classification models. Second, unlike general image classification tasks where category differences are typically reflected in large-scale visual features, ECG paper image classification heavily relies on subtle local patterns, such as a slight differences in wave morphology. These fine-grained details are essential for an accurate diagnosis, but are easily masked

by noise or lost during feature extraction.

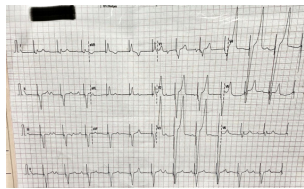
To solve these challenges, we propose a method that is designed for paper-ECG image classification. First, to deal with the noise and irrelevant information in the images, we introduce a data pre-processing pipeline. This pipeline helps to remove shadows, backgrounds, and other artefacts, so that the model can focus on the ECG waveforms. Second, to help the model better capture the small but important details in the ECG images, we propose a two-stage fine-tuning strategy. In the first stage, the model learns the domain-specific features of the ECG-like images using large synthetic datasets and several external ECG datasets. In the second stage, it is fine-tuned on our target dataset to improve its ability to recognise disease-related patterns. This method helps the model learn both the general patterns and the fine details needed for an accurate diagnosis.

## 2. Related Work

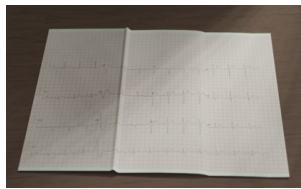
In this section, we outline previous work into generation of synthetic paper ECGs and classification of ECG images.

### 2.1. Generating Paper ECGs

To train deep learning models effectively, a large volume of high-quality training data is essential. However, due to the highly private nature of medical data, it is often difficult to obtain real-world ECG images. Even when such data are accessible, they often require a series of complex de-identification procedures to protect patient privacy. Meanwhile, large publicly-available ECG waveform datasets with cardiologist labels, such as PTB-XL [13], CPSC [14], and CODE15% [15], already exist. If these ECG waveform datasets could be leveraged to generate the corresponding ECG images, it would effectively address the challenge of acquiring sufficient training data.



(a) ECG Images generated by ecg-image-kit [16]



(b) ECG Images generated by GenECG [17]

Figure 1: ECG images generated by

The ecg-image-kit [16] and GenECG [17] are two generators that generate synthetic paper ECGs from ECG waveforms. Ecg-image-kit (Figure 1a) plots ECG waveforms on paper-like ECG backgrounds, followed by applying various distortions such as handwritten text artefacts, wrinkles, creases, and perspective transforms. GenECG

can generate images that provide images that visually appear similar to photographs of paper ECGs (Figure 1b). These images feature diverse backgrounds that mimic real-world tables and include artefacts such as shadows commonly observed in photographs. The GenECG images have passed a clinical Turing test in which expert observers could not distinguish between synthetic and real ECGs.

### 2.2. Classification of ECG Images

In the field of automatic interpretation of the ECG, apart from methods that focus on ECG waveforms, there is a number of work and questions about the classification of the ECG image.

There have been multiple previous attempts to interpret ECGs from images. These can be split into those that perform direct classification on the images, and those that first aim to extract and digitize the ECG signal. Work in this area has accelerated with the PhysioNet 2024 Challenge [18] and 2024 British Heart Foundation data science challenge. Both of these provided large labelled data sets of synthetically generated ECG images. We describe some of the key work below:

Among the **direct classification methods**, several studies focus on classifying individual heartbeat segments. Izci et al. [19] extracted single beats from the MIT-BIH arrhythmia database and transformed them into grayscale images, which were then classified using a LeNet-style CNN. Similarly, Jun et al. [20] resized heartbeat segments into 128×128 image patches and applied a VGG-like architecture to demonstrate the potential of deep learning for beat-level arrhythmia detection.

Other studies classify full 12-lead ECG images. Nawaz et al. [21] used a modified ResNet50 with Swish activations and custom dense layers to detect COVID-19-related cardiac abnormalities. Du et al. [22] extended the task to a multi-label setting using bilinear attention pooling to identify diagnostically relevant regions. Anwar et al. [23] demonstrated the effectiveness of data augmentation for improving robustness. Gliner et al. [24] introduced pixel-level gradient analysis via Jacobian matrices and domain-adversarial training to enhance both interpretability and generalisation. Mahmud et al. [25] proposed a multi-modal ensemble that integrates image-based and signal-based features. Dias et al. [26] applied transfer learning using ConvNeXt pre-trained on several ECG image datasets and fine-tuned on PTB-XL. Antoni et al. [27] proposed a two-stage architecture where an initial model estimates and corrects image rotation, followed by classification using a second ConvNeXt network.

In contrast, **signal extraction methods** aim to recover a digital ECG signal from the image prior to classification, reducing the impact of background textures, gridlines, and other visual artefacts. Gliner et al. [24] proposed a two-

stage framework that binarises smartphone-captured paper ECGs and applies a CNN for the classification of STEMI, LBBB, and RBBB. Chou et al. [28] used YOLOv7 to detect the signal region, followed by a CNN with self-attention to digitize the waveform, which was then classified using EfficientNet-B0. Yoon et al. [29] segmented waveform, grid, and text components using U-Net, reconstructed the signal with a rule-based algorithm, and classified it with RegNet. Summerton et al. [30] proposed a modular pipeline that extracts signals from full 12-lead paper ECG images using YOLOv7 and ResUNet, and classifies them with an ensemble SE-ResNet model.

### 3. Methods

In this work, our objective is to create a model that accurately classifies synthetic paper ECGs into 5 classes of clinical diagnoses. We first introduce the dataset used in this study, including its composition and characteristics. We then detail the data pre-processing steps applied to prepare the ECG images for model training. Subsequently, we outline the pretraining strategy designed to enhance model performance. Finally, we present the architecture of the proposed model and explain its key components.

The key novelty of this work is combining a noise-reducing pre-processing pipeline with a two-stage fine-tuning strategy, specifically designed for paper-ECG image classification. This combined approach enables the model to better focus on clinically relevant waveform details, even in the presence of common artefacts found in printed ECGs.

#### 3.1. Dataset

We used data from the BHF Data Science Centre ECG Challenge [31]. This dataset includes 21,799 12-lead ECG images generated from the PTB-XL waveform database [13] via the GenECG algorithm [17]. The images are displayed in the standard 3x4 layout. In total, 15,009 images are used as the training set, 3,219 images are used as the public validation set, and the remaining 3,219 images are reserved as a hidden test set. Each ECG image exhibited none, one, or multiple clinical diagnoses drawn from five categories. These include myocardial infarction (MI; a medical emergency due to blocked blood supply to the heart) [32], atrial fibrillation (AF; irregular and often rapid heartbeat with an absence of P-wave) [33], hypertrophy (HYP; enlargement of the heart muscle), conduction disturbance (CD; irregular electrical signaling), and ST/T changes (STTC; abnormal shifts in ECG wave patterns). Proportions of each class are summarised in Table 1.

Table 1: Number and proportion of positive and negative samples per diagnosis in the training set

	Diagnosis (n, %)
MI	3,819 (25.44%)
AF	1,033 (6.88%)
HYP	1,850 (12.33%)
CD	3,137 (20.90%)
STTC	3,640 (24.25%)

#### 3.2. Data Pre-processing Pipeline

As noted previously, the generated ECG images contain various types of noise, including various irrelevant backgrounds, artificial shadows, and simulated wrinkles and creases. To better extract meaningful information from the images and facilitate accurate classification by the model, we designed a data pre-processing pipeline, as illustrated in Figure 2.

First, we used a fine-tuned YOLO model [34] to localise the region corresponding to the paper ECG, followed by cropping of this rectangular region. We then applied the Segment Anything Model (SAM) [35] to more finely crop the paper ECG from the background. SAM provided co-ordinates corresponding to the four corners of the paper ECG. We applied a perspective transformation to convert the cropped ECG view to a canonical bird’s-eye perspective. Finally, we improve image contrast and colour distribution using the CLAHE (Contrast Limited Adaptive Histogram Equalisation) [36] algorithm.

#### 3.3. Model Architecture

We trained the model using ConvNeXt as the backbone [37]. ConvNeXt is a recent convolutional architecture that integrates design strengths from a range of state-of-the-art models, as illustrated in Figure 3. Specifically, ConvNeXt employs the widely used four-stage hierarchical design. Its stage depth ratio, notably improved and inspired by Swin-Transformer [38], utilises ratios of 1:1:3:1 or 1:1:9:1. Similarly to the Swin-Transformer, ConvNeXt introduces a stem layer that partitions the input image into patches, effectively reducing computational cost while efficiently capturing local features. Furthermore, ConvNeXt incorporates the principles of ResNeXt [39], integrating group convolutions and wider networks to achieve significantly better performance under comparable computational budgets. The model also leverages inverted bottleneck layers, inspired by MobileNetV2 [40], which are crucial to preserve information flow. Finally, ConvNeXt further benefits from the use of larger convolutional kernels, inspired by those from VGG networks [41], enhancing the receptive field and capturing richer contextual information.

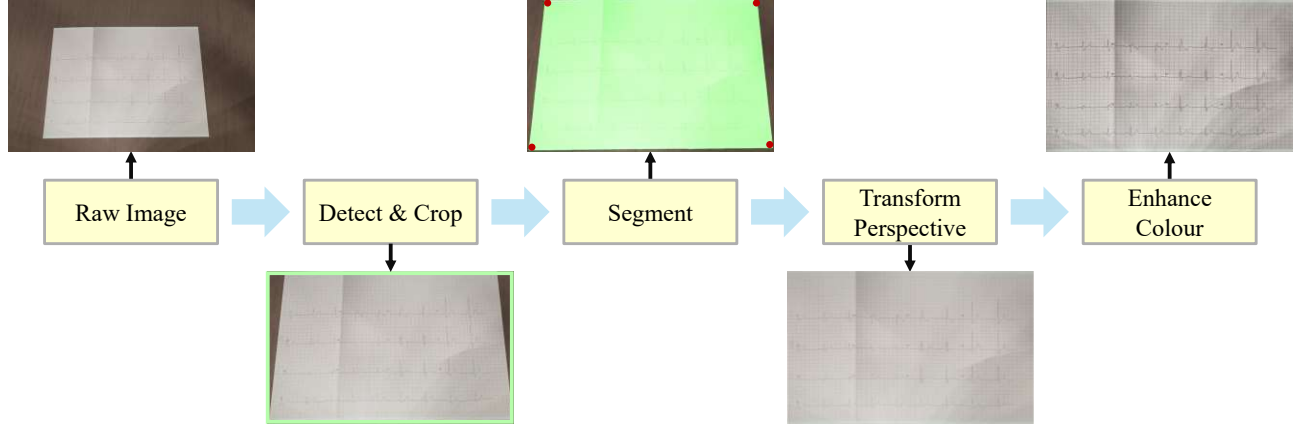


Figure 2: The data preprocessing pipeline. Step 1: raw image; Step 2: detection and cropping using YOLO; Step 3: segmentation using SAM; Step 4: perspective transformation to obtain a bird-eye view; Step 5: contrast enhancement using CLAHE. This pipeline effectively removes noise such as background clutter, shadows, and creases, and improves image quality to support model training.

For our experiments, we used the ConvNeXt-Base model implemented in the timm library [42]. The model was pre-trained on the ImageNet-22k dataset [43] and further fine-tuned on the ImageNet-1k dataset. The architecture hyperparameters for ConvNeXt-Base are as follows: channel dimensions  $C = (128, 256, 512, 1024)$  and number of blocks per stage  $B = (3, 3, 27, 3)$ .

### 3.4. Training Strategy

The Imagenet training data used to pre-train ConvNeXt contains a wide variety of images of common objects. In contrast, our task, paper ECG images, contain much less diversity; key disease-specific details are found only in the subtle morphology of the ECG waveforms. To address this domain gap, we designed a two-stage fine-tuning strategy:

**Stage I: Domain-Specific Fine-tuning** We assembled three external scanned ECG image datasets from Kaggle, including ECG Images by Pondy et al. [44], COVID-19 Detection Using ECG [45], and the National Heart Foundation 2023 ECG Dataset [46]. We also used GenECG [17] to convert the CODE15% waveform dataset [15] into synthetic paper-ECG images for additional domain-specific supervision.

During this stage, we fine-tuned ConvNeXt-Base for up to 50 epochs with a batch size of 32, using the AdamW optimiser [47] (learning rate  $1 \times 10^{-4}$ , weight decay  $1 \times 10^{-2}$ ). Early stopping with a patience of 5 epochs was applied to terminate training if no improvement was observed. A cosine-annealing learning rate schedule was applied, defined as

$$\lambda(\text{step}) = 0.5 (1 + \cos(2\pi \times \text{num\_cycles} \times \text{progress})),$$

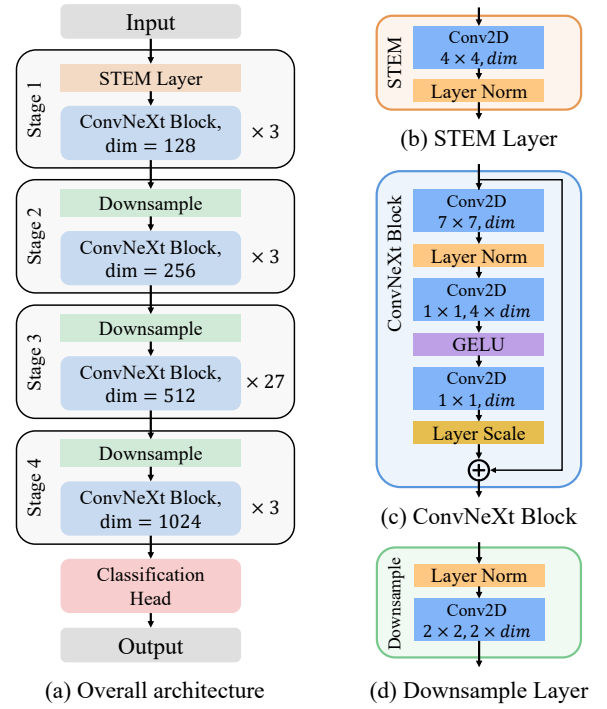


Figure 3: ConvNeXt Model Architecture and Key Modules. (a) Overall network structure. (b) Detail of the STEM Layer. (c) Internal structure of the ConvNeXt Block. (d) Components of the Downsample Layer.

where *progress* denotes the proportion of completed training steps and *num\_cycles* specifies the number of full sine wave periods (i.e. sine wave periods) within the learning rate schedule. Furthermore, to address class imbalance, we used a weighted binary cross-entropy loss, where the positive weights were calculated as the inverse of the positive rate for each label.

Data augmentation was performed using the Albumentations library [48]. We applied random rotations, elastic deformations, perspective transformations, and brightness/contrast adjustments. In addition, Catmull-Rom splines [49] were randomly applied to generate smooth curves that form polygonal masks that simulate shadows, further enriching the variability of the training data.

**Stage II: Task-Specific Fine-tuning** We then performed a five-fold cross-validation on the official BHF ECG Challenge training set. In each fold, the model was fine-tuned for 30 epochs with a reduced learning rate of  $1 \times 10^{-4}$ , batch size of 32, using the same AdamW setup, loss function (weighted binary cross-entropy loss with positive weights), and early stopping strategy (patience of 5 epochs) as in Stage I. Final predictions on the hidden test set were obtained through hard voting, by combining the outputs of the five models trained in cross-validation.

This two-stage approach allows ConvNeXt to first learn domain specific features from a diverse pool of paper-ECG-style images, and then specialise those features to the precise distribution and label set of the BHF challenge.

### 3.5. Metrics and Experimental setup

To find the best combination of model architecture and preprocessing pipeline, we performed a set of experiments.

In the first experiment, we compared ConvNeXt with other models, including ResNet, Vision Transformer, and Swin Transformer.

In the second experiment, we compared different data pre-processing strategies: no pre-processing, cropping only the ECG region, and fully segmenting the ECG from the background followed by a perspective transformation to generate a bird’s-eye view.

In the third experiment, we compared different model training strategies: (1) task-specific fine-tuning only, without any domain-specific adaptation; (2) a two-step approach involving domain-specific fine-tuning using synthetic data followed by task-specific fine-tuning; and (3) the full two-stage fine-tuning strategy.

To ensure fair comparisons across all experiments, we used the same fixed hyperparameters: a learning rate of  $1e-4$  with a decay factor of 0.5 applied every 7 epochs, a total of 30 training epochs, a dropout rate of 0.2, and a batch size of 32.

Once we had selected the best combination, we retrained the model and tuned the model hyperparameters.

To evaluate the performance of our model, we report the Area Under the Receiver Operating Characteristic Curve (AUROC).

All experiments were conducted on the Kaggle platform [50] using two NVIDIA T4 GPUs. Our implementation is based on the PyTorch framework [51] with the following software environment: Python 3.10.14, PyTorch 2.4.0, torchvision 0.19.0, scikit-learn 1.2.2, NumPy 1.26.4, pandas 2.2.3, timm 1.0.9, Pillow 10.4.0, wandb 0.18.3, and OpenCV 4.10.0.

Model training code is available at <https://github.com/Nicholas0917/BHF-Challenge-2024.git>

## 4. Results

The following results describe model performance on the BHF Challenge dataset, where the *Public Validation Set* refers to the data used for model validation during the competition, and the *Hidden Test Set* represents the data used after the competition to assess the final performance of the models. Neither the Public Validation Set or Hidden Test Set were used during training.

### 4.1. Model Selection

In the first experiment, we evaluated four representative deep learning architectures on the BHF Challenge dataset under identical training conditions. Table 2 summarises the AUROC performance of four representative deep learning models evaluated on the public validation and hidden test sets of the BHF Challenge dataset. These results demonstrate the performance of different architectures under the same experimental settings.

Table 2: Performance comparison of different models on the BHF Challenge dataset. AUROC scores are reported on the public validation and hidden test sets.

Model	Public Validation Set	Hidden Test Set
ResNet-50	0.7159	0.6997
ViT	0.8197	0.8209
Swin	0.8722	0.8675
ConvNeXt	<b>0.8750</b>	<b>0.8683</b>

### 4.2. Preprocessing selection

The second experiment assessed the impact of different pre-processing pipelines on model performance. As shown in Table 3, we compared three approaches: no pre-processing, cropping the ECG region only, and cropping combined with perspective transformation to generate a bird’s-eye view of the ECG paper.

Table 3: Evaluation of different ECG image preprocessing strategies. AUROC scores are reported on the public and hidden test sets.

Method	Public	Hidden
None	0.7703	0.7531
Crop Only	<b>0.8750</b>	<b>0.8683</b>
Segment & Perspective Transform	0.8359	0.8339

### 4.3. Training strategy selection

The third experiment explored different model training approaches to improve performance. We compared (i) task-specific fine-tuning only, (ii) fine-tuning with real ECG image data in the domain-specific fine-tuning stage, and (iii) the full two-stage fine-tuning strategy that incorporates both synthetic and real ECG data for domain-specific feature learning, as summarised in Table 4.

Table 4: Comparison of training strategies. AUROC scores are reported on the public and hidden test sets.

Setting	Public	Hidden
Task-specific fine-tuning only	0.8339	0.8172
Two-stage fine-tuning (only real ECG data in Domain-specific fine-tuning stage)	0.8677	<b>0.8729</b>
Two-stage fine-tuning (real + synthetic ECG data in Domain-specific fine-tuning stage)	<b>0.8750</b>	0.8683

### 4.4. Final tuned model

Based on the previous experimental results, we selected **ConvNeXt** as the model architecture, and adopted **cropping and contrast enhancement** as our data pre-processing pipeline. For the training strategy, we employed a **full two-stage fine-tuning** approach: the first stage involves pretraining on a combination of real and synthetic ECG data. It is worth noting that we conducted two separate experiments using different sources for the synthetic ECG data. In the first experiment, we used the CODE15% dataset to generate synthetic ECG images, which were then combined with real ECG images for the first stage of training. In the second experiment, we used the PTB-XL dataset as the source of synthetic ECG data, again combining the generated images with real ones for pretraining.

We further performed hyperparameter optimization based on this setup. The results after tuning are shown in Table 5.

Table 5: Final performance of the proposed model after hyperparameter optimization.

Model	Public	Hidden
Final Model (CODE15%)	0.9472	0.9430
Final Model (PTB-XL)	0.9688	0.9677

## 5. Discussion and Conclusions

Our experimental results highlight the crucial impact of three core components on the performance of ECG image classification: the choice of the backbone model, the design of the data pre-processing pipeline, and the training strategy.

First, as shown in Table 2, the selection of backbone architecture plays a decisive role. Among the evaluated models, ConvNeXt achieves the highest AUROC scores, outperforming ResNet-50, Vision Transformer (ViT), and Swin-Transformer.

Second, the design of the pre-processing pipeline (Table 3) has a non-negligible effect on performance. The results show that the model without pre-processing achieves the lowest AUROC scores, while applying a simple cropping operation that retains only the ECG region yields the best results. Introducing additional pre-processing, such as segmentation and perspective transformation, does not lead to further improvement. One possible explanation is that the evaluation data consist of synthetic ECG images, for which applying perspective distortion may disrupt the original geometric structure of the ECG. For example, the grid spacing in the background paper, often crucial for interpreting the waveform scale, may become inconsistent after transformation, introducing unnatural artefacts that confuse the model.

Third, the training strategy, particularly the proposed two-stage fine-tuning approach, is highly beneficial. As shown in Table 4, removing the first-stage adaptation or excluding synthetic data result in lower AUROC scores. This confirms that fine-tuning in diverse domain-relevant data (including synthetic examples) helps the model learn robust ECG-specific features before fine-tuning in the target data set.

Finally, we selected the optimal combination and performed hyperparameter tuning, achieving strong results, as shown in Table 5. Using synthetic ECG data generated from the PTB-XL dataset during the domain-specific fine-tuning stage yielded the best performance, surpassing the results obtained using synthetic data generated from CODE15%. However, since the dataset used in this challenge is also derived from PTB-XL, using PTB-XL as the source of synthetic ECG data for fine-tuning may introduce potential **data leakage**, which could lead to **overly optimistic** results.

Overall, our results demonstrate that the proposed data pre-processing pipeline, combined with the two-stage fine-tuning strategy, can effectively enhance the performance of classification on paper-like ECG images.

In future work, we plan to improve our model by exploring methods that are better at handling fine-grained image details. This will help the model better capture subtle shape differences in ECG images, which are often important for an accurate diagnosis.

## References

- [1] Martin SS, Aday AW, Almarzooq ZI, Anderson CAM, Arora P, Avery CL, et al. 2024 heart disease and stroke statistics: A report of us and global data from the american heart association. *Circulation An Official Journal of the American Heart Association* 2024;(8):149.
- [2] British Heart Foundation. Heart and circulatory disease statistics 2024: Compendium v3, October 2024. URL <https://www.bhf.org.uk/-/media/files/for-professionals/research/heart-statistics/bhf-cvd-statistics-compendium-2024-v3.pdf>. Accessed: 2025-07-12.
- [3] Somani S, Russak AJ, Richter F, Zhao S, Vaid A, Chaudhry F, et al. Deep learning and the electrocardiogram: review of the current state-of-the-art. *EP Europace* 2021;23(8):1179–1191.
- [4] Winters LJ, Till DA, Bing ML, Holmes JF. Time required for electrocardiogram interpretation in the emergency department. *Academic Emergency Medicine* 2022;29(5).
- [5] Wasimuddin M, Elleithy K, Abuzneid AS, Faezipour M, Abuzaghlh O. Stages-based ecg signal analysis from traditional signal processing to machine learning approaches: A survey. *IEEE Access* 2020;8:177782–177803.
- [6] Khurshid S, Friedman S, Reeder C, Di Achille P, Diamant N, Singh P, et al. Ecg-based deep learning and clinical risk factors to predict atrial fibrillation. *Circulation* 2022; 145(2):122–133.
- [7] Pourbabaee B, Roshtkhari MJ, Khorasani K. Deep convolutional neural networks and learning ecg features for screening paroxysmal atrial fibrillation patients. *IEEE Transactions on Systems Man and Cybernetics Systems* 2017; 48(12):2095–2104.
- [8] Gao J, Li Y, Chen M, Zhang X, Sun Y, Jiang X, et al. Efficient transformation of ecg signals from 1-d to 2-d for atrial fibrillation detection using deep learning. *Signal Image and Video Processing* 2025;19(9):1–19.
- [9] Baloglu UB, Talo M, Yildirim O, San Tan R, Acharya UR. Classification of myocardial infarction with multi-lead ecg signals and deep cnn. *Pattern recognition letters* 2019; 122:23–30.
- [10] Acharya UR, Fujita H, Oh SL, Hagiwara Y, Tan JH, Adam M. Application of deep convolutional neural network for automated detection of myocardial infarction using ecg signals. *Information sciences* 2017;415:190–198.
- [11] Sannino G, De Pietro G. A deep learning approach for ecg-based heartbeat classification for arrhythmia detection. *Future Generation Computer Systems* 2018;86:446–455.
- [12] Wu H, Patel KHK, Li X, Zhang B, Galazis C, Bajaj N, et al. A fully-automated paper ecg digitisation algorithm using deep learning. *Scientific Reports* 2022;12(1):20963.
- [13] Wagner P, Strodthoff N, Bousseljot RD, Kreiseler D, Lunze FI, Samek W, et al. PTB-XL, a Large Publicly Available Electrocardiography Dataset. *Scientific Data* 2020;7(1):1–15.
- [14] Liu F, Liu C, Zhao L, Zhang X, Wu X, Xu X, et al. An Open Access Database for Evaluating the Algorithms of Electrocardiogram Rhythm and Morphology Abnormality Detection. *Journal of Medical Imaging and Health Informatics* 2018;8(7):1368–1373.
- [15] Ribeiro AH, Paixao G, Lima EM, Ribeiro MH, Pinto Filho MM, Gomes PR, et al. Code-15%: A large scale annotated dataset of 12-lead ecgs. *Zenodo* Jun 2021;9:10–5281.
- [16] Shivashankara KK, Shervedani AM, Clifford GD, Reyna MA, Sameni R, et al. Ecg-image-kit: a synthetic image generation toolbox to facilitate deep learning-based electrocardiogram digitization. *Physiological measurement* 2024; 45(5):055019.
- [17] Bodagh N, Tun KS, Barton A, Javidi M, Rashid D, Burns R, et al. Genecg: A synthetic image-based ecg dataset to augment artificial intelligence-enhanced algorithm development. *BMJ Health Care Informatics* 2025;32(1):e101335.
- [18] Reyna MA, Deepanshi WJ, Koscova Z, Elola A, Seyedi S, Campbell K, et al. Digitization and classification of ecg images: The george b. moody physionet challenge 2024. *Computing in Cardiology* 2024;51:1–4.
- [19] Izci E, Ozdemir MA, Degirmenci M, Akan A. Cardiac arrhythmia detection from 2d ecg images by using deep learning technique. In *2019 medical technologies congress (TIPTEKNO)*. IEEE, 2019; 1–4.
- [20] Jun TJ, Nguyen HM, Kang D, Kim D, Kim YH. Ecg arrhythmia classification using a 2-d convolutional neural network. *arXiv preprint arXiv180406812* 2018;.
- [21] Nawaz M, Saleem S, Masood M, Rashid J, Nazir T. Covid-ecg-rsnet: Covid-19 classification from ecg images using swish-based improved resnet model. *Biomedical Signal Processing and Control* 2024;89:105801.
- [22] Du N, Cao Q, Yu L, Liu N, Zhong E, Liu Z, et al. Fm-ecg: A fine-grained multi-label framework for ecg image classification. *Information Sciences* 2021;549:164–177.
- [23] Anwar T, Zakir S. Effect of image augmentation on ecg image classification using deep learning. In *2021 International Conference on Artificial Intelligence (ICAI)*. IEEE, 2021; 182–186.
- [24] Gliner V, Levy I, Tsutsui K, Acha MR, Schliamser J, Schuster A, et al. Clinically meaningful interpretability of an ai model for ecg classification. *NPJ Digital Medicine* 2025; 8(1):109.
- [25] Mahmud T, Barua A, Islam D, Hossain MS, Chakma R, Barua K, et al. Ensemble deep learning approach for ecg-based cardiac disease detection: Signal and image analysis. In *2023 International Conference on Information and Communication Technology for Sustainable Development (ICICT4SD)*. IEEE, 2023; 70–74.

- [26] Dias FM, Ribeiro E, Soares QB, Krieger JE, Gutierrez MA. Image-based electrocardiogram classification using pre-trained convnext. In 2024 Computing in Cardiology (CinC); .
- [27] Antoni L, Bruoth E, Bugata P, Jr PB, Gajdoš D, Hudák D, et al. Digital signal and image-based ecg classification and its performance by modern residual convolutional networks. In 2024 Computing in Cardiology (CinC); .
- [28] Chou CT, González S. Dual deep learning system to digitize and classify 12-lead ecgs from scanned images. In 2024 Computing in Cardiology (CinC); .
- [29] Yoon HC, Kim DK, Kim HS, Seo WY, Heo CH, Kim SH. Segmentation-based extraction of key components from ecg images: A framework for precise classification and digitization; .
- [30] Summerton S, Dinsdale N, Leinonen T, Searle G, Kaisti M, Wong DC. A modular framework for the interpretation of paper ecgs. In Proceedings of 51st International Computing in Cardiology Conference, volume 51. Computing in Cardiology, 2024; .
- [31] Centre BDS. Bhf data science centre ecg challenge. <https://kaggle.com/competitions/bhf-data-science-centre-ecg-challenge>, 2024. Kaggle.
- [32] BHF. Heart attack, 2023. URL <<https://www.bhf.org.uk/information-support/conditions/heart-attack>>.
- [33] BHF. Atrial fibrillation (af), 2023. URL <<https://www.bhf.org.uk/information-support/conditions/atrial-fibrillation>>.
- [34] Redmon J, Divvala S, Girshick R, Farhadi A. You only look once: Unified, real-time object detection. In Proceedings of the IEEE conference on computer vision and pattern recognition. 2016; 779–788.
- [35] Kirillov A, Mintun E, Ravi N, Mao H, Rolland C, Gustafson L, et al. Segment anything. In Proceedings of the IEEE/CVF international conference on computer vision. 2023; 4015–4026.
- [36] Reza AM. Realization of the contrast limited adaptive histogram equalization (clahe) for real-time image enhancement. Journal of VLSI signal processing systems for signal image and video technology 2004;38:35–44.
- [37] Liu Z, Mao H, Wu CY, Feichtenhofer C, Darrell T, Xie S. A convnet for the 2020s. In Proceedings of the IEEE/CVF conference on computer vision and pattern recognition. 2022; 11976–11986.
- [38] Liu Z, Lin Y, Cao Y, Hu H, Wei Y, Zhang Z, et al. Swin transformer: Hierarchical vision transformer using shifted windows. In Proceedings of the IEEE/CVF international conference on computer vision. 2021; 10012–10022.
- [39] Xie S, Girshick R, Dollár P, Tu Z, He K. Aggregated residual transformations for deep neural networks. In Proceedings of the IEEE conference on computer vision and pattern recognition. 2017; 1492–1500.
- [40] Sandler M, Howard A, Zhu M, Zhmoginov A, Chen LC. Mobilenetv2: Inverted residuals and linear bottlenecks. In Proceedings of the IEEE conference on computer vision and pattern recognition. 2018; 4510–4520.
- [41] Simonyan K, Zisserman A. Very deep convolutional networks for large-scale image recognition. arXiv preprint arXiv:1409.1556 2014;.
- [42] Wightman R. Pytorch image models. <https://github.com/rwightman/pytorch-image-models>, 2019.
- [43] Deng J, Dong W, Socher R, Li LJ, Li K, Fei-Fei L. Imagenet: A large-scale hierarchical image database. In 2009 IEEE conference on computer vision and pattern recognition. Ieee, 2009; 248–255.
- [44] Pondy J. Cardiovascular ecg images, 2023. URL <<https://www.kaggle.com/datasets/jayaprakashpondy/ecgimages>>.
- [45] Khan AH, Hussain M, Malik MK. Ecg images dataset of cardiac and covid-19 patients. Data in Brief 2021; 34:106762.
- [46] Foundation NH. National heart foundation 2023 ecg dataset — kaggle, 2023. URL <<https://www.kaggle.com/drkhaledmohsin/national-heart-foundation-2023-ecg-dataset>>.
- [47] Loshchilov I, Hutter F. Decoupled weight decay regularization. arXiv preprint arXiv:1711.05101 2017;.
- [48] Buslaev A, Iglovikov VI, Khvedchenya E, Parinov A, Druzhinin M, Kalinin AA. Albumentations: Fast and flexible image augmentations. Information 2020;11(2). ISSN 2078-2489. URL <https://www.mdpi.com/2078-2489/11/2/125>.
- [49] Twigg C. Catmull-rom splines. Computer 2003;41(6):4–6.
- [50] Kaggle. Kaggle: Your machine learning and data science community, 2023. URL <<https://www.kaggle.com/>>.
- [51] Imambi S, Prakash KB, Kanagachidambaresan G. Pytorch. Programming with TensorFlow solution for edge computing applications 2021;87–104.

Address for correspondence:

David Wong  
Level 10, Worsley Building, University of Leeds, Leeds, United Kingdom  
wmqn2362@leeds.ac.uk